THE JOURNAL OF BIOLOGICAL CHEMISTRY VOL. 284, NO. 21, pp. 14396–14404, May 22, 2009

Oxidative Stress Is Linked to ERK1/2-p16 Signaling-mediated Growth Defect in ATM-deficient Astrocytes*

Received for publication, October 22, 2008, and in revised form, March 25, 2009 Published, JBC Papers in Press, March 25, 2009, DOI 10.1074/jbc.M808116200

Jeesun Kim and Paul K. Y. Wong[1]

From the Department of Carcinogenesis, University of Texas M. D. Anderson Cancer Center, Smithville, Texas 78957

The gene that encodes the ATM protein kinase is mutated in ataxia-telangiectasia (A-T). One of the prominent features of A-T is progressive neurodegeneration. We have previously reported that primary astrocytes isolated from $Atm^{-/-}$ mice grow slowly and die earlier than control cells in culture. However, the mechanisms for this remain unclear. We show here that intrinsic elevated intracellular levels of reactive oxygen species (ROS) are associated with the senescence-like growth defect of $Atm^{-/-}$ astrocytes. This condition is accompanied by constitutively higher levels of ERK1/2 phosphorylation and $p16^{Ink4a}$ in $Atm^{-/-}$ astrocytes. We also observe that ROS-induced up-regulation of $p16^{Ink4a}$ occurs correlatively with ERK1/2-dependent down-regulation and subsequent dissociation from chromatin of Bmi-1. Furthermore, both mitogen-activated protein kinase (MAPK)/ERK inhibitor PD98059 and antioxidant *N*-acetyl-L-cysteine restored normal proliferation of $Atm^{-/-}$ astrocytes. These results suggest that ATM is required for normal astrocyte growth through its ability to stabilize intracellular redox status and that the inability to control ROS is the molecular basis of limited cell growth of $Atm^{-/-}$ astrocytes. This defect may be mediated by a mechanism involving ERK1/2 activation and Bmi-1 derepression of $p16^{Ink4a}$. These data identify new potential targets for therapeutic intervention in A-T neurodegeneration.

A prominent feature of ataxia-telangiectasia (A-T)[2] is neurodegeneration that is caused by mutations in the *Atm* (ataxia-telangiectasia mutated) gene (1–3). The *Atm* gene product, ATM protein kinase, regulates the cell cycle in response to DNA damage and to oxidative stress (4, 5). Within the central nervous system (CNS), proper responses to ROS are required to prevent neurodegeneration (6–9). Others have shown that exogenous antioxidants prevent Purkinje cell death (10) and correct neurobehavioral deficits in $Atm^{-/-}$ mice (11, 12). These findings suggest that abnormalities in redox status contribute to the A-T phenotype (13–16). Although increased oxidative stress has been shown to characterize ATM deficiency in the CNS, the mechanisms by which oxidative stress promotes neuronal cell loss in A-T remain unclear.

A-T neurodegeneration is primarily due to a loss of cerebella Purkinje neurons and to malfunction of other neuronal cells as well (3). Neurons in the CNS depend upon astrocytes for structural, functional, and thiol support (17, 18). For example, Purkinje neurons in the cerebellum rely heavily on their supporting Bergmann astrocytes (19). We have shown that Bergmann astrocytes of $Atm^{-/-}$ mice are under oxidative stress (20), implying that oxidative stress resulting from a loss of ATM may promote astrocyte dysfunction. Others have also shown that cultured astrocytes from $Atm^{-/-}$ mice have cell cycle and growth defects (21) and that astrocytes isolated from $Atm^{-/-}$ mouse embryos grow poorly in culture and readily undergo senescence (15, 20). These observations imply that ATM is essential for normal astrocyte growth and maturation. In light of the importance of astrocytes in supporting neurons against oxidative stress, we hypothesize that aberrant growth and function of $Atm^{-/-}$ astrocytes may contribute to neuron loss in A-T.

We show here that $Atm^{-/-}$ astrocytes exhibit senescence-like growth arrest, compared with the growth characteristics of their wild type ($Atm^{+/+}$) counterparts. We also show that elevated ROS levels are one of the causes of proliferation defects in $Atm^{-/-}$ astrocytes. This conclusion is based on the observation that defective cell growth of $Atm^{-/-}$ astrocytes is restored to normal by the antioxidant *N*-acetyl-L-cysteine (NAC). This in turn implies that the role of ATM in normal astrocytic proliferation involves stabilization of redox status in the cell. We also observe that growth arrest of $Atm^{-/-}$ astrocytes is associated with chronic maintenance of high levels of the cyclin-dependent kinase inhibitors and phosphorylation of ERK1/2 under conditions in which intracellular ROS levels are elevated. In addition, we identify an intermediate player, Bmi-1, that links ERK1/2 to up-regulation of $p16^{Ink4a}$. Bmi-1, apolycomb group protein, has been implicated in proliferation of several cell types, through its transcriptional repression of $p16^{Ink4a}$ (22, 23). We observe that ROS-induced Bmi-1 down-regulation and dissociation from chromatin are both ERK1/2-dependent. This suggests that the up-regulation of $p16^{Ink4a}$ is mediated by a mechanism involving ERK1/2 activation and Bmi-1 loss-of-function as transcription repressor of $p16^{Ink4a}$. Finally, we show that the MEK inhibitor PD98059 reverses $p16^{Ink4a}$ up-regulation and chromatin dissociation of Bmi-1. Furthermore, knockdown of $p16^{Ink4a}$ greatly corrected the cell growth defect in $Atm^{-/-}$ astrocytes. These studies identify a role of ATM in controlling normal astrocyte growth and maturation. This is

* This work was supported by a fellowship from the Odyssey Program of M. D. Anderson Cancer Center (to J. K.) and by funds from the Longevity Foundation and Ataxia-telanglectasia (A-T) Children's Project.

[1] To whom correspondence should be addressed: The University of Texas, M. D. Anderson Cancer Center, Science Park-Research Division, 1808 Park Rd., 1C, P.O. Box 389, Smithville, TX 78957. Tel.: 512-237-9456; Fax: 512-237-2444; E-mail: pkwong@mdanderson.org.

[2] The abbreviations used are: A-T, ataxia-telangiectasia; H_2DCFDA, 2′-7′-dichlorofluorescene diacetate; ERK, extracellular signal-regulated kinase; MAPK, mitogen-activated protein kinase; NAC, *N*-acetyl-L-cysteine; SA, senescence-associated; ROS, reactive oxygen species; MEK, MAPK/ERK kinase; CNS, central nervous system; PBS, phosphate-buffered saline; siRNA, small interfering RNA; CDK, cyclin-dependent kinase(s); Rb, retinoblastoma.

carried out by suppression of oxidative stress-dependent signaling pathways.

EXPERIMENTAL PROCEDURES

Mice—$Atm^{-/-}$ mice were originally generated by C. Barlow (24). For this study, they were purchased from the Jackson Laboratories (Bar Harbor, ME). We genotyped offspring ($Atm^{+/+}$, $Atm^{+/-}$, or $Atm^{-/-}$) by real time polymerase chain reaction-based assays of mouse tail DNA. Littermates were used as controls in all of the experiments. Animal care was in accordance with the University of Texas M. D. Anderson Cancer Center guidelines for animal experiments.

Cells and Cell Culture—Immortalized murine C1 astrocytes were maintained in Dulbecco's modified Eagle's medium supplemented with 10% fetal bovine serum and antibiotics (100 units/ml penicillin and 100 μg/ml streptomycin) (25). The cells were passaged biweekly and used for experiments while in the exponential growth phase. Primary astrocytes were isolated from 1–2-day-old newborn mouse pups by a method described previously (20, 26). Whole brain of each newborn mouse was removed and minced separately in ice-cold Dulbecco's modified Eagle's medium/F-12 medium. A single-cell suspension was obtained by passing the minced tissue through a 70-m nylon mesh cell strainer. The cells were plated onto poly-L-lysine-coated 10-mm flasks and grown in Dulbecco's modified Eagle's medium/F-12 medium, supplemented with 10% fetal bovine serum, 5 units/ml penicillin, 5 μg/ml streptomycin, and 2.5 g/ml Fungizone. The cells were cultured for 4 days in an incubator with 5% CO_2 atmosphere at 37 °C until reaching confluence. They were passaged by trypsinization. Cells from passage 4 or 5 were used for all experiments. Astrocytes by the fourth or fifth passage were >99% glial fibrillary acidic protein (GFAP)-positive (27).

Chemical Reagents—ATM inhibitor KU55933 (10 μM) was purchased from Sigma. MEK inhibitor PD98059 (50 μM) was purchased from BD Biosciences, and antioxidant NAC (1 mM) was kindly provided by M. Yan (M. D. Anderson Cancer Center) (28).

Analysis of Cell Senescence—SA β-galactosidase assay kit (Cell Signaling) was used to visualize senescent cells. Astrocytes were cultured in 6-well plates for 2 days and then fixed after being washed twice with PBS. The cells were further incubated for 24 h in the presence of staining solution-containing 5-bromo-4-chloro-3-indolyl-β-D-galactopyranoside (X-gal). Senescent cells were distinguished from viable cells using β-galactosidase, which is blue under the microscope.

Analysis of Intracellular ROS—Intracellular ROS accumulation was monitored by using 2′-7′-dichlorofluorescene diacetate (H_2DCFDA), which forms a fluorescent compound, dichlorofluorescein, upon oxidation with ROS. After 30 min of incubation in 10 μM H_2DCFDA, the cells were rinsed twice with PBS. Fluorescence was monitored by scanning the whole well using a NucleoCounter (New Brunswick Scientific Co., Ltd.) set at excitation and emission wavelengths of 485 and 535 nm.

Protein Analysis—The cells ($1–5 \times 10^6$) were seeded into 10-cm dishes, grown to 70% confluence, and treated with H_2O_2 at different concentrations. At 1, 4, or 16 h after H_2O_2 treatment, the cells were washed twice with ice-cold PBS and then scraped directly into lysis buffer containing 150 mM NaCl, 0.5% w/v SDS, 0.5% v/v Nonidet P-40, 0.5% w/v sodium deoxycholate, 1 mM EGTA, and a mixture of protease inhibitors (Complete Mini tablets; Roche Applied Science). Protein concentrations were determined using a Bradford reagent (Bio-Rad). The protein lysates (30 μg) were separated by SDS-polyacrylamide gel electrophoresis on a 12% gel and transferred to polyvinylidene difluoride membrane. Antibodies used for Western blotting analysis were anti-ERK1/2, anti-phospho-ERK1/2 (Thr^{202}/Tyr^{204}), anti-phospho-Rb ($Ser^{807/811}$), anti-PCNA, and anti-$p27^{kip1}$ (Cell Signaling Technology); anti-Bmi-1 (Upstate Biotechnology); anti-$p21^{cip1}$, anti-$p16^{Ink4a}$, and anti-actin (Santa Cruz Biotechnology).

siRNA-mediated Knockdown—For siRNA knockdown of *Atm*, the cells were transfected for 48 h with 20 nM siRNA (mouse-specific *Atm*) in medium containing 10% (v/v) fetal bovine serum using Lipofectamine reagent (Invitrogen) according to the manufacturer's protocol for cells. Validated siRNA (SMARTpool) was obtained from Dharmacon. The negative control siRNA used was siCONTROL, which contains at least four mismatches to all known human, mouse, and rat genes. For mock transfection, we used siRNA suspension buffer and Lipofectamine containing no siRNA. For siRNA knockdown of $p16^{Ink4a}$, mouse-specific $p16^{Ink4a}$ siRNA was purchased from Santa Cruz Biotechnology.

Immunofluorescence—The cells were fixed with 4% paraformaldehyde in PBS for 30 min at room temperature and then permeabilized with 0.1% Triton X-100 in PBS for 15 min. For staining with antibodies, the cells were incubated for 2 h at 37 °C with 10% fetal bovine serum in PBS. Primary antibodies were added, and the cells were incubated at 4 °C overnight. The cells were then washed three times in PBS, 0.1% Triton X-100 for 5 min each, and fluorescent secondary antibodies were added for 1 h at 37 °C. The nuclei were stained with 4′,6-diamidino-2-phenylindole, and the slides were mounted in Slowfade (Molecular Probes). The cells were imaged under an Olympus IX2-SL microscope equipped with a ×400 objective and an Olympus DP 70 digital camera connected to a PC computer.

Statistics—For each experiment, the data are presented as the means ± S.D. of values. Each experiment was repeated at least three times. Statistical comparisons of values for $Atm^{+/+}$ *versus* $Atm^{-/-}$ mice and for untreated control *versus* treated samples were made using the Mann-Whitney *U* test. The differences were considered significant when $p < 0.05$.

RESULTS

Loss of ATM Impairs Proliferation in Astrocytes—We have reported previously that ATM-deficient primary astrocytes grow slowly, become senescent, and die in culture (20). These results are consistent with those reported by Gosink *et al.* (21). To compare the rate of proliferation of $Atm^{+/+}$ and $Atm^{-/-}$ astrocytes, we analyzed their cell growth curves. As shown in Fig. 1*A*, $Atm^{-/-}$ astrocytes proliferated much more slowly than $Atm^{+/+}$ astrocytes. In particular, $Atm^{+/+}$ astrocytes show 2.5–3 times higher rates of proliferation than $Atm^{-/-}$ astrocytes at 4 and 5 days after subculturing. When monolayer of $Atm^{+/+}$ and $Atm^{-/-}$ astrocytes were observed under the

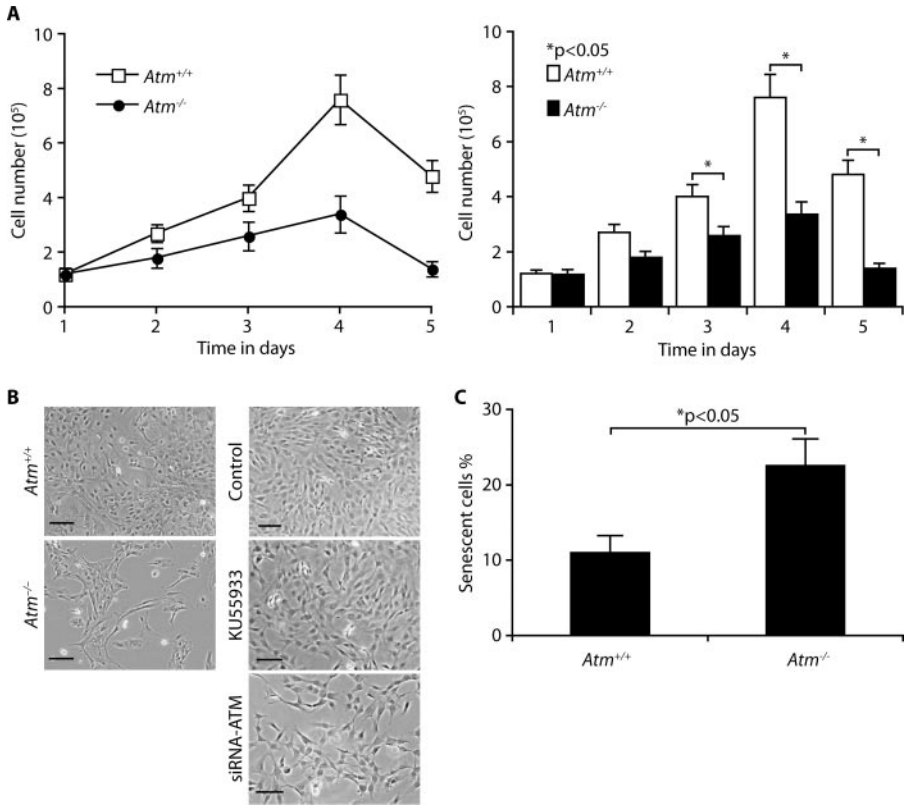

FIGURE 1. **Loss of ATM impairs proliferation in astrocytes.** *A*, astrocytes were isolated from the brains of newborn $Atm^{+/+}$ and $Atm^{-/-}$ mice, and their growth curves were determined by trypan blue staining at indicated days after initial seeding of cells. The means ± S.D. of three independent experiments are shown. *, $p < 0.05$ when $Atm^{-/-}$ astrocytes were compared with $Atm^{+/+}$ astrocytes. *B*, phase contrast photomicrographs of $Atm^{+/+}$ and $Atm^{-/-}$ astrocytes following further incubation for 4 days (*left panel*). ATM in C1 astrocytes was inactivated by ATM inhibitor KU55933, and knocked down using ATM siRNA (*right panel*). *Scale bars*, 50 μm. *C*, the proportions of senescent cells in $Atm^{+/+}$ and $Atm^{-/-}$ astrocytes were determined by SA β-galactosidase expression 2 days after cultivation. The means ± S.D. of three independent experiments are shown. *, $p < 0.05$ when $Atm^{-/-}$ astrocytes were compared with $Atm^{+/+}$ astrocytes.

microscope following further incubation for 4 days, $Atm^{-/-}$ astrocytes showed lower densities than wild type control cells with a decrease of ~50% in cell number (Fig. 1*B*, *left panel*). This is consistent with our findings for C1 astrocytes, a murine immortalized astrocyte cell line (25). Although the ATM inhibitor KU55933 slightly decreases astrocytes proliferation, the loss of ATM by ATM siRNA reduced cell proliferation by ~40% (Fig. 1*B*, *right panel*). To obtain direct evidence that ATM deficiency causes cell senescence, a specific SA β-galactosidase assay was performed after 2 days of culture. Fig. 1*C* shows that senescent cells are present two times more in $Atm^{-/-}$ astrocyte cultures than $Atm^{+/+}$ cultures. These data indicate that ATM deficiency causes the senescent-like cell growth defect in $Atm^{-/-}$ astrocytes.

Decreased Proliferation in $Atm^{-/-}$ Astrocytes Is Caused by Elevated ROS Levels—ATM monitors cellular redox status in addition to its monitoring of DNA damage and genomic instability (26), and cells lacking ATM show ROS accumulation (16). Although we have previously shown that a loss of *Atm* results in oxidative damage in the brain (20), the involvement of oxidative stress in defective astrocyte growth in the ATM-deficient mouse has not been tested. To address this issue, we compared intracellular ROS levels in $Atm^{+/+}$ and $Atm^{-/-}$ astrocytes by H_2DCFDA staining of intracellular H_2O_2. The data show that the intracellular levels of ROS are significantly higher in $Atm^{-/-}$ astrocytes than in $Atm^{+/+}$ astrocytes and that antioxidant NAC reduces the elevated ROS levels of $Atm^{-/-}$ astrocytes to normal levels (Fig. 2*A*). This result suggests that elevated ROS levels are intrinsic characteristics of cells lacking ATM. This is consistent with our results from C1 astrocytes treated with ATM-specific inhibitor, KU55933, which show higher levels of intracellular ROS compared with untreated control cells (data not shown). For direct evidence that defective proliferation of $Atm^{-/-}$ astrocytes is due to elevated ROS levels, we treated $Atm^{-/-}$ astrocytes with NAC and compared their proliferation rates to those of untreated cells. Fig. 2*B* shows that proliferation rates for $Atm^{-/-}$ astrocytes were increased by treatment with NAC, showing nearly 2–2.5 times higher rates than untreated $Atm^{-/-}$ counterpart at 3 and 4 days after subculturing. This effect of NAC was confirmed by photomicrograph, which disclosed increased cell density by NAC (Fig. 2*C*). This is consistent with our findings that NAC decreases the proportion of senescent cells in $Atm^{-/-}$ astrocyte cultures (Fig. 2*D*). These results provide strong evidence linking defective growth of $Atm^{-/-}$ astrocytes to elevated intracellular ROS.

H_2O_2-treated $Atm^{+/+}$ Astrocytes Show Reduced Proliferation and Up-regulated Levels of CDK Inhibitors—To determine whether H_2O_2 decreases $Atm^{+/+}$ astrocyte proliferation and whether antioxidant inhibits ROS-mediated defective proliferation in normal $Atm^{+/+}$ astrocytes subjected to exogenous oxidative stress, we exposed $Atm^{+/+}$ astrocytes to H_2O_2 and treated the same H_2O_2-exposed cells with NAC. Fig. 3*A* shows that H_2O_2 elevated intracellular ROS levels in $Atm^{+/+}$ astrocytes and that treatment of $Atm^{+/+}$ astrocytes with NAC reduced their intracellular ROS to normal levels. $Atm^{+/+}$ astrocytes also showed significantly decreased proliferation 2 days after H_2O_2 treatment, but H_2O_2-induced defective proliferation was partially restored by NAC (Fig. 3*B*). Treatment with H_2O_2 for 2 days followed by 1 day of incubation in H_2O_2-free medium induced SA β-galactosidase expression in ~40% of $Atm^{+/+}$ astrocytes, but NAC significantly prevented H_2O_2-induced senescence (Fig. 3*C*). These results indicate that H_2O_2 inhibits astrocytes proliferation through elevating intracellular ROS, regardless of their ATM status.

We then investigated the effects of ROS on several known key intermediates associated with cell proliferation. The inhib-

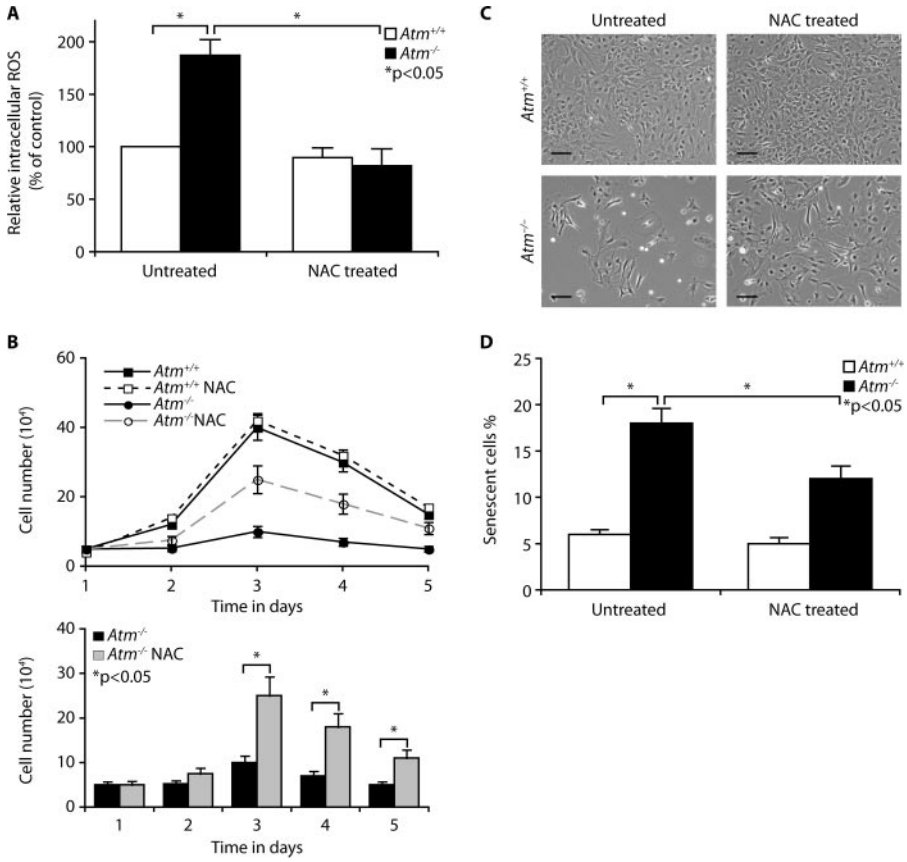

FIGURE 2. **Decreased proliferation in $Atm^{-/-}$ astrocytes is caused by elevated ROS levels.** *A*, $Atm^{+/+}$ and $Atm^{-/-}$ astrocytes were either left untreated or pretreated with NAC (1 mM) for 2 h. Fluorescent H_2DCFDA levels were determined for these cells. The means ± S.D. of three independent experiments are shown. *, $p < 0.05$ when untreated $Atm^{-/-}$ culture were compared with untreated $Atm^{+/+}$ astrocytes or when NAC-treated $Atm^{-/-}$ astrocytes were compared with untreated $Atm^{-/-}$ astrocytes. *B*, growth curves of $Atm^{-/-}$ astrocytes in the presence or absence of NAC (1 mM) were analyzed for 5 days and then compared with those of $Atm^{+/+}$ astrocytes. The means ± S.D. of three independent counting are shown. *, $p < 0.05$ when NAC-treated $Atm^{-/-}$ astrocytes were compared with untreated $Atm^{-/-}$ astrocytes. *C*, photomicrographs of $Atm^{+/+}$ and $Atm^{-/-}$ astrocytes in the presence or absence of NAC. *Scale bars*, 50 μm. *D*, senescence of $Atm^{+/+}$ and $Atm^{-/-}$ astrocytes in the presence or absence of NAC was compared by SA β-galactosidase expression 2 days after cultivation. The means ± S.D. of three independent experiments are shown. *, $p < 0.05$ when untreated $Atm^{-/-}$ culture was compared with untreated $Atm^{+/+}$ astrocytes or when NAC-treated $Atm^{-/-}$ astrocytes was compared with untreated $Atm^{-/-}$ astrocytes.

itors of cyclin-dependent kinases (CDK) are considered to play an important role in cell cycle arrest and premature senescence (30). Others have shown that the CDK inhibitor $p21^{cip1}$ is up-regulated in $Atm^{-/-}$ astrocytes (26). Therefore, we investigated the effects of ROS on levels of CDK inhibitors, including $p16^{Ink4a}$, $p19^{Arf}$, $p21^{cip1}$, and $p27^{kip1}$ in $Atm^{+/+}$ astrocytes. H_2O_2 treatment of $Atm^{+/+}$ astrocytes stimulated expression of $p21^{cip1}$ and $p16^{Ink4a}$, but not $p27^{kip1}$ in $Atm^{+/+}$ astrocytes (Fig. 3*D*, *upper* and *lower panels*). However, no $p19^{Arf}$ band was present in the lysates from those cells. These alterations indicate that activation of the $p16^{Ink4a}$ and/or $p19^{Arf}$-$p21^{cip1}$ senescence pathway(s) may be involved in ROS-mediated senescence in astrocytes. Furthermore, activation of $p16^{Ink4a}$ was attenuated by NAC (Fig. 3*E*). These findings suggest that intracellular ROS-mediated oxidative stress induces senescence in astrocytes via activation of the $p16^{Ink4a}$ pathway.

In $Atm^{-/-}$ Astrocytes, ERK1/2 Is Constitutively Activated, and CDK Inhibitors Are Up-regulated—We have previously reported that ERK1/2 is activated in both $Atm^{-/-}$ astrocytes in culture and in Bergmann glia in the cerebella of $Atm^{-/-}$ mice (20). We consistently observed higher level of phospho-ERK1/2 in $Atm^{-/-}$ astrocytes than in $Atm^{+/+}$ astrocytes. In addition, Bmi-1, a polycomb ring finger oncogene product, is down-regulated in $Atm^{-/-}$ cells (Fig. 4*A*), which is consistent with the fact that Bmi-1 promotes cell proliferation via repression of CDK inhibitors. In Fig. 3*D*, we have shown that intracellular ROS levels increased in $Atm^{-/-}$ astrocytes, and H_2O_2 up-regulated CDK inhibitors. We therefore reasoned that CDK inhibitors might be up-regulated to decrease proliferation in $Atm^{-/-}$ astrocytes. We thus compared the basal levels of CDK inhibitors in $Atm^{-/-}$ astrocytes with those in wild type control cells. Fig. 4*B* shows that the basal expression levels of p53, $p21^{cip1}$, and $p16^{Inka}$ were higher in $Atm^{-/-}$ cells than in the wild type cells. $p16^{Ink4a}$ was up-regulated $Atm^{-/-}$ cerebella tissues. Not surprisingly, $Atm^{-/-}$ astrocytes show lower levels of retinoblastoma (Rb) phosphorylation than do wild type control cells. Moreover, Bmi-1 levels were significantly down-regulated in the $Atm^{-/-}$ tissues (Fig. 4*C*, *left* and *right panels*).

We next compared $p16^{Ink4a}$ levels in $Atm^{-/-}$ astrocytes and $Atm^{+/+}$ astrocytes, to which exogenous H_2O_2 had been added. Interestingly, the addition of H_2O_2 caused a brief up-regulation of $p16^{Inka}$ at 4 h in wild type control cells but then reversed itself down to the untreated basal level at 16 h post-treatment. However, when $Atm^{-/-}$ astrocytes were exposed to H_2O_2, the level of $p16^{Ink4a}$ expression was further elevated, and this up-regulation persisted from 4 to 16 h post-H_2O_2 treatment. This means that oxidative stress caused by elevated ROS is reversible to normal levels when ATM kinase is present. In both $Atm^{+/+}$ and $Atm^{-/-}$ astrocytes, Bmi-1 was down-regulated in response to H_2O_2, but its level was lower in $Atm^{-/-}$ astrocytes than in $Atm^{+/+}$ astrocytes (Fig. 4*D*). In $Atm^{+/+}$ astrocytes, the brief expression of $p16^{Ink4a}$ may shut down cell cycling, allowing time for the cells to repair any damage. Once the job is done, their levels return to normal, as a result of the redox balancing action of ATM.

Fig. 4*E* shows that in both $Atm^{+/+}$ and $Atm^{-/-}$ astrocytes, H_2O_2 treatment also causes phosphorylation of ERK1/2 and up-regulation of $p16^{Ink4a}$. Phospho-ERK1/2 and $p16^{Ink4a}$ changes that occurred in H_2O_2-treated $Atm^{+/+}$ astrocytes were less pronounced than in H_2O_2-treated $Atm^{-/-}$ astrocytes. $Atm^{-/-}$ astrocytes also show lower levels of Rb phosphoryla-

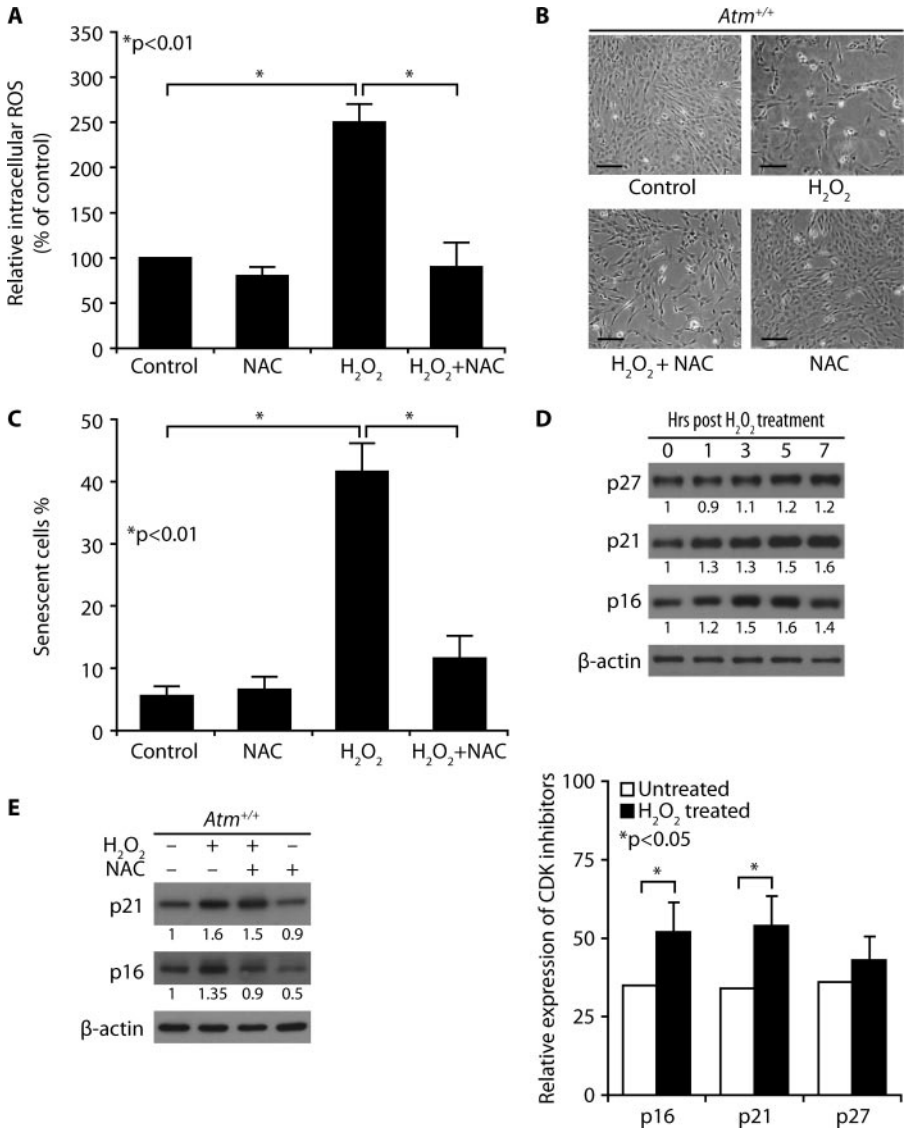

FIGURE 3. **H_2O_2-treated $Atm^{+/+}$ astrocytes show reduced proliferation and up-regulated levels of CDK inhibitors.** *A*, $Atm^{+/+}$ astrocytes were pretreated with 1 mM NAC before treatment with 100 μM H_2O_2. Intracellular ROS levels were then measured in cultures. The means ± S.D. of three independent experiments are shown. *, $p < 0.01$ when H_2O_2-treated $Atm^{+/+}$ astrocytes was compared with untreated $Atm^{+/+}$ culture or when NAC- and H_2O_2-treated $Atm^{+/+}$ astrocytes were compared with H_2O_2-treated $Atm^{+/+}$ culture. *B*, $Atm^{+/+}$ astrocytes were pretreated with 1 mM NAC before treating with 100 μM H_2O_2. Photomicrographs were taken following a subsequent 4-day incubation. *Scale bars*, 50 μm. *C*, SA β-galactosidase expressions in cultures from the experiment shown in *A*. The means ± S.D. of three independent experiments are shown. *, $p < 0.01$ when H_2O_2-treated $Atm^{+/+}$ culture was compared with untreated $Atm^{+/+}$ culture or when NAC- and H_2O_2-treated $Atm^{+/+}$ culture was compared with H_2O_2-treated $Atm^{+/+}$ culture. *D*, $Atm^{+/+}$ astrocytes were treated with 100 μM H_2O_2, and then levels of $p27^{kip1}$, $p21^{cip1}$, and $p16^{Ink4a}$ were determined. The means ± S.D. of three independent experiments are shown. *, $p < 0.05$ when H_2O_2-treated $Atm^{+/+}$ astrocytes were compared with untreated $Atm^{+/+}$ astrocytes. *E*, the effects of NAC on $p21^{cip1}$ and $p16^{Ink4a}$ expressions were determined by direct Western blotting analysis after H_2O_2 treatment in the presence of NAC.

tion than do wild type control cells. Moreover, Rb phosphorylation was further reduced after H_2O_2 exposure. These results indicate that $Atm^{-/-}$ astrocytes are differentially hypersensitive to oxidative stress and maintain high expression levels of phospho-ERK1/2 and $p16^{Ink4a}$. If oxidative stress is prolonged, as it is in cells lacking ATM, up-regulation of phospho-ERK1/2 persistently may increase $p16^{Ink4a}$ expression, resulting in prolonged cell cycle arrest and retardation of cell proliferation. These data strongly implicate the involvement of ERK1/2-$p16^{Ink4a}$ signaling pathway in ROS-induced cell growth arrest of $Atm^{-/-}$ astrocytes.

ERK1/2 Signaling Mediates Bmi-1 Down-regulation and Chromatin Dissociation in $Atm^{-/-}$ Astrocytes—We next set out to identify the molecular mechanisms underlying the effects of ROS on the cell growth defects of $Atm^{-/-}$ astrocytes, focusing on the mechanisms for phospho-ERK1/2 and $p16^{Ink4a}$ up-regulation. $p16^{Ink4a}$ expression is known to be regulated by the MAPK pathways, including activation of ERK1/2 (31). Furthermore, exposure to H_2O_2 activates MAPKs in many cell types (32, 33). Therefore, we tested the effect of ROS on ERK1/2 downstream mediators. Upon phosphorylation at two amino acids (Thr^{202}/Tyr^{204}), ERK1/2 translocates into the nucleus, where it phosphorylates its substrates. Because $p16^{Ink4a}$ expression level does not depend on phosphorylation by ERK1/2, it is not a direct substrate of activated ERK1/2. Instead, $p16^{Ink4a}$ expression is negatively regulated by Bmi-1 (34). Amino acid sequence analysis indicates that Bmi-1 has two predicted consensus motifs for ERK1 phosphorylation. We thus asked whether ROS-induced ERK1/2 signaling has effects on Bmi-1 function as a transcription repressor for $p16^{Ink4a}$.

The polycomb group proteins including Bmi-1 function as transcription repressors. Chromatin association of these proteins can be demonstrated by puncta in the nucleus in previous study (35). Immunofluorescence imaging of endogenous Bmi-1 in $Atm^{+/+}$ astrocytes indicates that Bmi-1 localizes mainly in chromatin and that it dissociates from chromatin after cells are exposed to H_2O_2 with a concomitant up-regulation of $p16^{Ink4a}$ (Fig. 5*A*). Bmi-1/chromatin association correlates with trimethylation at the lysine 27 residue of histone H3 (H3K27me3; data not shown), because H3K27me3 is required for polycomb/histone H3 interaction (36). However, it was also noted that Bmi-1/chromatin association does not correlate with sites of DNA double strand breaks, because fluorescence images of 53BP1 did not colocalize with Bmi-1 in astrocytes treated with H_2O_2 (Fig. 5*B*).

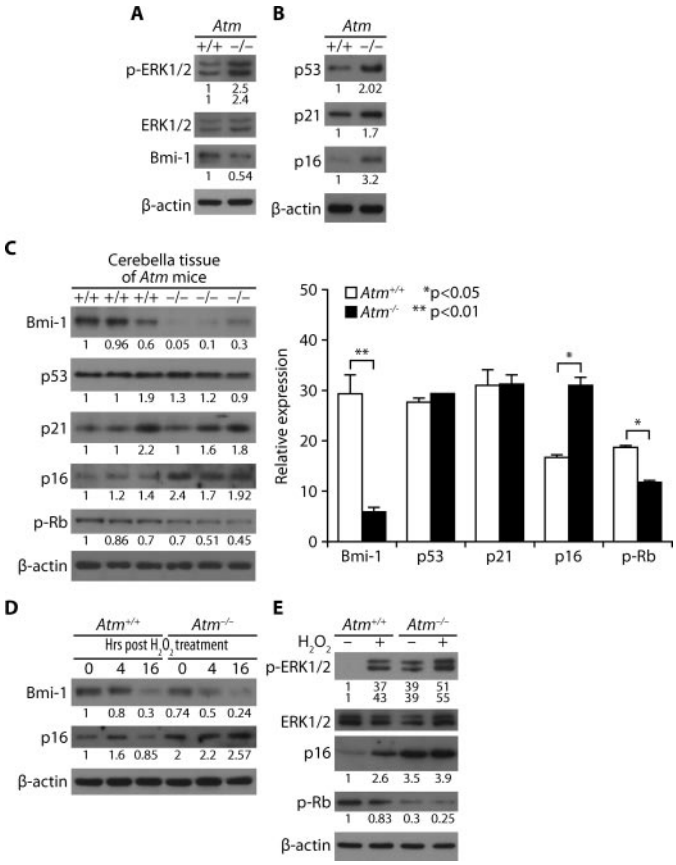

FIGURE 4. **In $Atm^{-/-}$ astrocytes, ERK1/2 is constitutively activated and CDK inhibitors are up-regulated.** *A* and *B*, for $Atm^{+/+}$ and $Atm^{-/-}$ astrocytes, levels of phospho-ERK1/2, ERK1/2, and Bmi-1 (*A*) and levels of p53, $p21^{cip1}$, and $p16^{Ink4a}$ (*B*) were assessed by direct Western blotting analysis. *C*, levels of Bmi-1, p53, $p21^{cip1}$, $p16^{Ink4a}$, and phospho-Rb were compared for $Atm^{+/+}$ and $Atm^{-/-}$ cerebella tissues by direct Western blotting analysis. The means ± S.D. of three different mice tissues are shown. *, $p < 0.05$; **, $p < 0.01$ when $Atm^{-/-}$ tissues was compared with $Atm^{+/+}$ tissues. *D*, $Atm^{+/+}$ and $Atm^{-/-}$ astrocytes were treated with 100 μM H_2O_2. The cells were then harvested to access levels of Bmi-1 and $p16^{Ink4a}$ at the indicated times after H_2O_2 treatment. *E*, $Atm^{+/+}$ and $Atm^{-/-}$ astrocytes were either left untreated or treated with 100 μM H_2O_2. Levels of phospho-ERK1/2, ERK1/2, $p16^{Ink4a}$, and phospho-Rb were determined by direct Western blotting analysis.

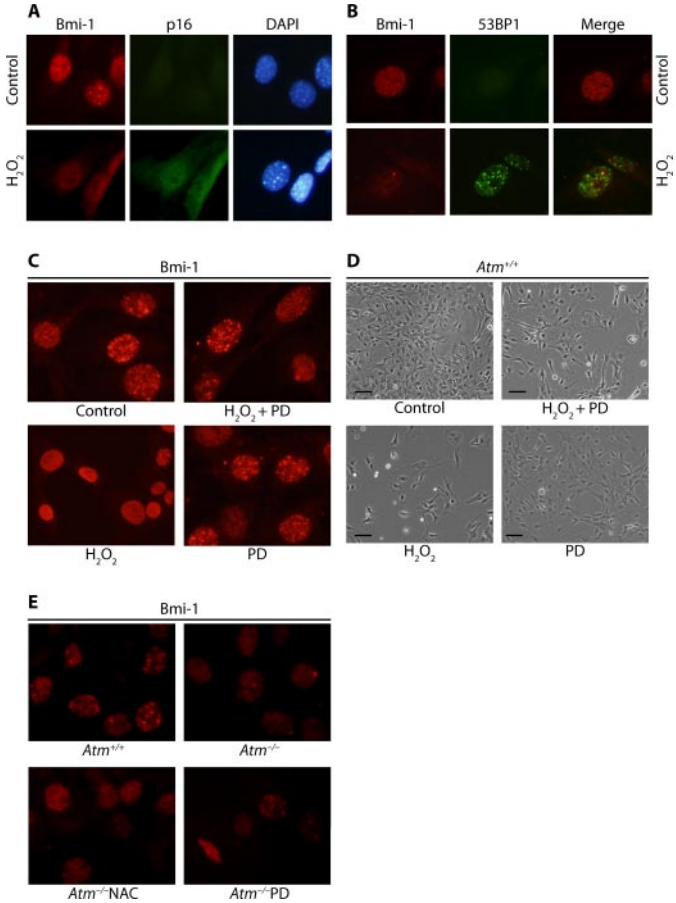

FIGURE 5. **ERK1/2 signaling mediates Bmi-1 down-regulation and chromatin dissociation in $Atm^{-/-}$ astrocytes.** *A*, $Atm^{+/+}$ astrocytes were synchronized by contact inhibition after subculture, at which time cells were treated with 100 μM H_2O_2. Bmi-1 association with chromatin was analyzed by fluorescence microscope for the presence of puncta in the nucleus. $p16^{Ink4a}$ up-regulation and Bmi-1/chromatin dissociation was tested using anti-$p16^{Ink4a}$ antibody. *B*, colocalization of Bmi-1 and 53BP1 was tested in the cells after H_2O_2 treatment using the same methods. *C*, $Atm^{+/+}$ astrocytes were left untreated or pretreated with 50 μM PD98059 (*PD*) overnight, before treating with 100 μM H_2O_2. The effects of 50 μM PD98059 on Bmi-1 localization in astrocytes were analyzed. *D*, photomicrographs of $Atm^{+/+}$ astrocytes culture from the experiment shown in *C*. *Scale bars*, 50 μm. *E*, $Atm^{-/-}$ astrocytes were treated with 1 mM NAC or 50 μM PD98059 for 2 days. Bmi-1 expression and localization in $Atm^{+/+}$ and $Atm^{-/-}$ astrocytes were determined. *DAPI*, 4′,6-diamidino-2-phenylindole.

We next asked whether H_2O_2-induced Bmi-1/chromatin dissociation is dependent on ERK1/2 signaling. We thus pretreated $Atm^{+/+}$ astrocytes with MEK inhibitor PD98059 before H_2O_2 treatment, because MEK is known as the upstream of ERK1/2 (32). Fig. 5*C* shows that H_2O_2-induced Bmi-1/chromatin dissociation is significantly inhibited by PD98059. This suggests that Bmi-1 dissociation from chromatin occurs via ERK1/2 signaling. In addition, H_2O_2 inhibits astrocyte proliferation, but PD98059 partially rescues it (Fig. 5*D*). Taken together with increased proliferation by PD98059, reversion of chromatin dissociation and restoration of Bmi-1 by PD98059 indicate that H_2O_2-induced proliferation decrease is associated to Bmi-1 dysfunction by ERK1/2 signaling.

Next, we assessed the effect of ATM deficiency on endogenous Bmi-1 localization using $Atm^{-/-}$ astrocytes. Fig. 5*E* shows that Bmi-1 is down-regulated, and less Bmi-1 associate with chromatin in $Atm^{-/-}$ astrocytes than in $Atm^{+/+}$ astrocytes. (NAC and PD98059 partially restored levels of Bmi-1 expression and chromatin association in $Atm^{-/-}$ astrocytes). These results are consistent with previous findings of Bmi-1 down-regulation and $p16^{Ink4a}$ up-regulation that occur in $Atm^{-/-}$ astrocytes (Fig. 4*A*). The data link $p16^{Ink4a}$ up-regulation to Bmi-1 down-regulation in $Atm^{-/-}$ astrocytes and in turn also link these two events to elevated intracellular ROS levels. Because PD98059 also restored normal Bmi-1 and $p16^{Ink4a}$ levels in $Atm^{-/-}$ astrocytes, we conclude that ERK1/2 mediates Bmi-1 down-regulation and chromatin dissociation, as well as $p16^{Ink4a}$ up-regulation.

Restoration of Normal Proliferation of $Atm^{-/-}$ Astrocytes by Inactivation of ERK1/2 Signaling or Knockdown of $p16^{Ink4a-}$— We next asked whether activation of ERK1/2 impairs survival and proliferation of $Atm^{-/-}$ astrocytes and whether inhibiting ERK1/2 signaling restores defective cell growth. We established cultures of $Atm^{-/-}$ astrocytes in the presence of PD98059. Growth curve analysis for 5 days showed that PD98059 partially rescued $Atm^{-/-}$ astrocytes from defective proliferation (Fig. 6*A*). The restorative actions of PD98059 were also evident in

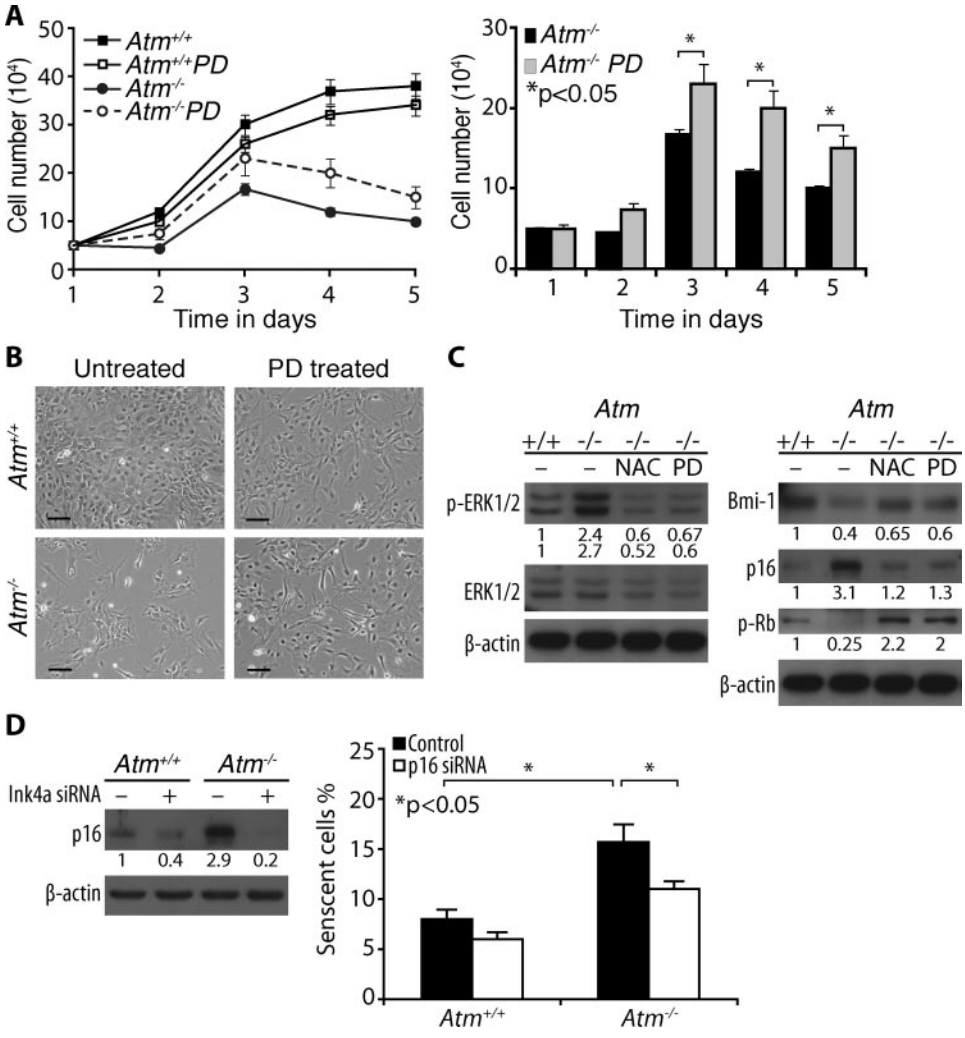

FIGURE 6. **Restoration of normal proliferation of $Atm^{-/-}$ astrocytes by inactivation of ERK1/2 signaling or knockdown of $p16^{Ink4a}$.** *A*, growth curves of $Atm^{+/+}$ and $Atm^{-/-}$ astrocytes, cultured either in the presence or absence of 50 μM PD98059. PD98059 partially rescued $Atm^{-/-}$ astrocytes from defective proliferation. The means ± S.D. of three independent countings are shown. *, $p < 0.05$ when PD98059-treated $Atm^{-/-}$ astrocytes were compared with untreated $Atm^{-/-}$ astrocytes. *B*, photomicrographs of $Atm^{+/+}$ and $Atm^{-/-}$ astrocytes culture in the presence or absence of PD98059. *Scale bars*, 50 μm. *C*, $Atm^{+/+}$ astrocytes were left untreated. $Atm^{-/-}$ astrocytes were either untreated left or treated with 1 mM NAC or 50 μM PD98059 for 2 days. The levels of phospho-ERK1/2, ERK1/2, Bmi-1, $p16^{Ink4a}$, and phospho-Rb were determined by direct Western blotting analysis. *D*, $Atm^{+/+}$ and $Atm^{-/-}$ astrocytes were transfected with Ink4a siRNA. $p16^{Ink4a}$ levels were determined by direct Western blotting analysis (*left panel*). Proportions of senescent cells were determined by SA β-galactosidase expression 2 days after cultivation (*right panel*). The means ± S.D. of three independent experiments are shown. *, $p < 0.05$ when untransfected $Atm^{-/-}$ astrocytes were compared with untransfected $Atm^{+/+}$ culture or when Ink4a siRNA-transfected $Atm^{-/-}$ astrocytes were compared with untransfected $Atm^{-/-}$ astrocytes.

culture, as shown by increase in cell density (Fig. 6*B*). However, the positive effect of PD98059 on proliferation of $Atm^{-/-}$ astrocytes was not comparable with that of the antioxidant NAC. In addition, PD98059 appeared to inhibit mitogenic pathways in $Atm^{+/+}$ astrocytes, because it reduced growth rate and proliferation in these cells. In normal $Atm^{+/+}$ mice, most astrocytes are quiescent, and thus ERK1/2 signaling is suspended in an inactive state. However, $Atm^{-/-}$ astrocytes maintain constitutive ERK1/2 signaling associated with oxidative stress conditions.

Despite its inhibitory effect on $Atm^{+/+}$ astrocytes proliferation, PD98059 partially restored Bmi-1 levels in $Atm^{-/-}$ astrocytes. In addition, both NAC and PD98059 reduced levels of $p21^{cip1}$ and $p16^{Ink4a}$ in $Atm^{-/-}$ astrocytes to levels similar to those in $Atm^{+/+}$ astrocytes. In accordance with these results, level of phospho-Rb was also increased by NAC and PD98059 (Fig. 6*C*). These results provide direct evidence linking defective growth of $Atm^{-/-}$ astrocytes to activation of ERK1/2 signaling as a result of oxidative stress. However, PD98059 has modest and partial rescuing effect on $Atm^{-/-}$ astrocytes proliferation, indicating that there may be additional pathways associated with defective proliferation in $Atm^{-/-}$ astrocytes.

Because increases in cell senescence and $p16^{Ink4a}$ level were observed in $Atm^{-/-}$ astrocytes, we next decided to access whether $p16^{Ink4a}$ up-regulation is responsible for inducing cell senescence and whether inhibition of $p16^{Ink4a}$ expression would reverse the defective growth phenotype of $Atm^{-/-}$ astrocytes. Ink4a was knocked down in both $Atm^{+/+}$ and $Atm^{-/-}$ astrocytes using siRNA against mouse $p16^{Ink4a}$. Fig. 6*D* shows that more senescent cells were observed in $Atm^{-/-}$ astrocytes than in $Atm^{+/+}$ astrocytes. However, $Atm^{-/-}$ astrocytes when $p16^{Ink4a}$ was knocked down had fewer senescent cells than did the cells whose $p16^{Ink4a}$ was intact.

DISCUSSION

In A-T patients, Purkinje neuron loss in the cerebellum is the most critical feature of the neuropathological phenotype (37). Up to now, therefore, most studies have focused on the effects of ATM deficiency in neurons, with the role(s) of astrocytes going unexplored. However, accumulating evidence now suggests that astrocytes are key elements serving pivotal functions in the central nervous system, including structural and redox support for neuron, neurotransmitter synthesis, and transport of nutrients and metabolic precursors to neurons (17, 19, 38–40). Previous studies have reported that transgenic and knock-out mouse models for certain astrocyte-specific proteins result in neurodegenerative disorders (41, 42). This implies that abnormalities in astrocytes might also cause neuropathophysiology of A-T. This is consistent with earlier observations by others that Purkinje cell survival in *Atm*-deficient mice is partially reversed when these cells are cultured in the presence of $Atm^{+/+}$ astrocyte-conditioned medium (18). It will be important now to determine whether $Atm^{-/-}$ astrocytes have cytotoxic

effects for neurons in coculture. Studies now in progress in our lab will address the effects of $Atm^{-/-}$ astrocytes on neurons in this context.

At normal concentrations, ROS play a role in cellular functions involving signal transduction (43, 44). However, an imbalance between generation of ROS and capacity of antioxidants to neutralize ROS can result in disruption of cellular redox status, leading to oxidative stress (45–47). Mammalian cells have therefore evolved a wide range of mechanisms, including ATM, for maintaining normal levels of intracellular ROS. Neuronal cells require large quantities of oxygen to function because of their high metabolic rate. As a result, neurons generate high levels of ROS. For this reason, the CNS is very vulnerable to ROS imbalance and accumulation. In general, low doses of H_2O_2 promote cell proliferation, whereas high levels of ROS elicit cell cycle arrest, senescence, and apoptosis (48). Our data show that $Atm^{-/-}$ astrocytes have a lower proliferation rate than that of normal cells. We previously observed increased spontaneous DNA synthesis in cultured $Atm^{-/-}$ astrocytes relative to $Atm^{+/+}$ astrocyte despite their decreased proliferation (20). The reason for this discrepancy is unknown. However, it is possible that abnormally elevated DNA synthesis in $Atm^{-/-}$ astrocytes may occur without cell division. This is in turn could elevate ROS production in the cells (15).

Our observations that $p21^{cip1}$ is up-regulated in $Atm^{-/-}$ astrocytes (Fig. 4*B*) and that PD98059 inhibits $p21^{cip1}$ up-regulation (data not shown) are consistent with those from a previous study (26). The *Ink4a/Arf* locus encodes two proteins, $p16^{Ink4a}$ and $p19^{Arf}$, by alternative splicing (49–51). *Ink4a* and *Arf* are important components in Rb and p53 pathways, respectively, and both proteins function in cell cycle regulation (52, 53). Bmi-1 is a potent repressor of both *Ink4a* and *Arf*. Our data suggest that Bmi-1 down-regulation and dissociation from chromatin with resultant $p16^{Ink4a}$ up-regulation may contribute to the defective proliferation and premature senescence of $Atm^{-/-}$ astrocytes. A very interesting observation made by other researchers is that *Bmi-1* knock-out mice progressively develop A-T-like motor abnormalities, such as ataxia (22). This information substantiates the observations reported above and supports the idea that CNS pathology is similar if either ATM or Bmi-1 is absent. Because derepression of the Ink4a/Arf gene locus has been correlated with *Bmi-1*-deficient phenotypes in the nervous system, it is important to determine whether the deletion of both *Ink4a* and *Arf* genes restores functions of $Atm^{-/-}$ astrocytes. Notably, we observed that knockdown of Ink4a restores proliferation of $Atm^{-/-}$ astrocytes (Fig. 6*D*). Furthermore, work by others has also shown that the A-T like motor abnormalities observed in *Bmi-1* knock-out mice restored in $Bmi\text{-}1^{-/-}/p16^{Ink4a-/-}$ double knock-out mice (54). This result further substantiates that $p16^{Ink4a}$ plays a role in *Bmi-1*-deficient conditions.

We have shown that Bmi-1/chromatin association is disrupted by H_2O_2 (Fig. 5, *A–C*). Previous studies on Bmi-1 have reported that its function as transcription repressor is regulated by its phosphorylation status (35). Because Bmi-1 contains two predicted ERK1 phosphorylation sites, we asked whether Bmi-1 phosphorylation is induced by oxidative stress and whether it is ERK1/2 dependent. We reasoned that ROS-induced phosphorylation of Bmi-1 may directly or indirectly contribute to its chromatin dissociation, which in turn would result in derepression of $p16^{Ink4a}$. Because no specific antibody is available to detect the phosphorylated form of Bmi-1, its phosphorylation was determined by mobility shift on gels in the presence of phosphatase inhibitors. These experiments demonstrated that H_2O_2 treatment causes the mobility shift of Bmi-1 (data not shown). However, even though down-regulation and chromatin dissociation of Bmi-1 occur in $Atm^{-/-}$ astrocytes, no intrinsic difference in Bmi-1 phosphorylation is observed between $Atm^{+/+}$ and $Atm^{-/-}$ astrocytes in Western blotting analysis (Fig. 4*A*). This might be explained by the fact that the mobility shift of Bmi-1 is able to be detected for only short time after H_2O_2 treatment, after which time Bmi-1 levels decreased (Fig. 4*D*). Therefore, it is possible that phosphorylation of Bmi-1 may lead to its degradation. It will be interesting to determine whether inhibition of proteasomal degradation restores functions of $Atm^{-/-}$ astrocytes by preventing Bmi-1 degradation.

In recent years, accumulating evidence has indicated that protein kinase activities are redox-sensitive because key cysteine residues in these proteins can undergo post-translational modifications by oxidants. H_2O_2-induced formation of disul-

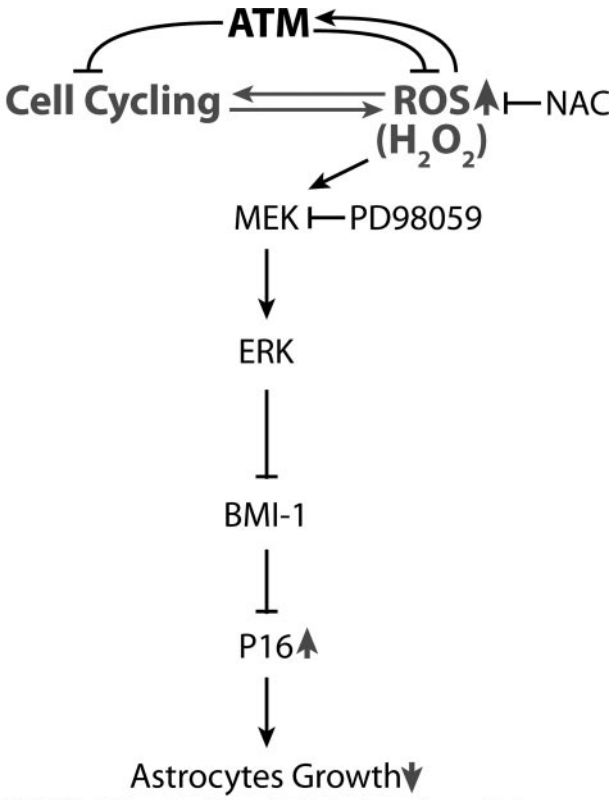

FIGURE 7. **Proposed model of a role for ATM in the maintenance of normal astrocyte proliferation.** ATM is necessary to control intracellular levels of ROS. In the absence of ATM, elevated levels of ROS elicit oxidative stress and limited growth of astrocytes, through multiple ERK1/2-dependent mechanisms, including down-regulation and chromatin dissociation of Bmi-1, as well as up-regulation of $p16^{Ink4a}$. Abnormal proliferation of $Atm^{-/-}$ astrocytes may lead to oxidative stress in entire central nervous system and eventually to neurodegeneration. Oxidative stress-mediated growth defects of $Atm^{-/-}$ astrocytes may be prevented by antioxidants, and normal astrocyte proliferation may be partially restored by inhibition of ERK1/2 signaling. The *arrows* denote an increase or decrease when ATM is absent.

fide bonds in protein kinases has been documented, suggesting that kinases function as redox sensors and that H_2O_2-induced conformational changes or formation of dimers from disulfide bonds triggers kinase activation (45, 55). This is consistent with our observation that ATM is activated in response to H_2O_2 (data not shown). Although at present the mechanism of how H_2O_2-induced ERK1/2 activation is unclear, we speculate that a candidate upstream mediator, such as receptor tyrosine kinase may be responsible for H_2O_2-induced ERK1/2 activation, because others have shown that upstream receptor tyrosine kinase may act as a trigger for such events (29). Our further studies will address the role of receptor tyrosine kinase in modulating H_2O_2-induced ERK1/2 signaling.

In conclusion, our data demonstrate that ATM is required to maintain normal growth of astrocytes by controlling intracellular levels of ROS. The absence of ATM limits the growth of astrocytes through ERK1/2-dependent mechanisms, including down-regulation and chromatin dissociation of Bmi-1 and subsequent up-regulation of p16^{Ink4a}. The events are prevented by antioxidants and inhibited by inactivation of MEK, which is upstream of ERK1/2 (Fig. 7). These data therefore identify a novel mechanism by which ATM deficiency leads to the astrocytes growth arrest, and they identify new targets for effective pharmacological intervention in A-T patients.

Acknowledgments—We thank Lifang Zhang for providing excellent technical support for the astrocyte cultures and Atm mouse preparation and Mingshan Yan (M. D. Anderson Cancer Center) for kindly providing advice and the antioxidant NAC. We also thank Virginia Scofield for careful reading of the manuscript.

REFERENCES

1. Savitsky, K., Bar-Shira, A., Gilad, S., Rotman, G., Ziv, Y., Vanagaite, L., Tagle, D. A., Smith, S., Uziel, T., Sfez, S., Ashkenazi, M., Pecker, I., Frydman, M., Harnik, R., Patanjali, S. R., Simmons, A., Clines, G. A., Sartiel, A., Gatti, R. A., Chessa, L., Sanal, O., Lavin, M. F., Jaspers, N. G., Taylor, A. M., Arlett, C. F., Miki, T., Weissman, S. M., Lovett, M., Collins, F. S., and Shiloh, Y. (1995) *Science* **268,** 1749–1953
2. Jorgensen, T. J., and Shiloh, Y. (1996) *Int. J. Radiat. Biol.* **69,** 527–537
3. Crawford, T. O. (1998) *Semin. Pediatr. Neurol.* **5,** 287–294
4. Shiloh, Y., and Rotman, G. (1996) *J. Clin. Immunol.* **16,** 254–260
5. Shiloh, Y. (2003) *Nat. Rev. Cancer* **3,** 155–168
6. Lucius, R., and Sievers, J. (1996) *Brain Res.* **743,** 56–62
7. Campese, V. M., Ye, S., Zhong, H., Yanamadala, V., Ye, Z., and Chiu, J. (2004) *Am. J. Physiol.* **287,** 695–703
8. Leutner, S., Schindowski, K., Frölich, L., Maurer, K., Kratzsch, T., Eckert, A., and Müller, W. E. (2005) *Parmacopsychiatry* **38,** 312–315
9. Jiang, Y., Scofield, V. L., Yan, M., Qiang, W., Liu, N., Reid, A. J., Lynn, W. S., and Wong, P. K. (2006) *J. Virol.*, **80,** 4557–4569
10. Chen, P., Peng, C., Luff, J., Spring, K., Watters, D., Bottle, S., Furuya, S., and Lavin, M. F. (2003) *J. Neurosci.* **23,** 11453–11460
11. Browne, S. E., Roberts, L. J., II, Dennery, P. A., Doctrow, S. R., Beal, M. F., Barlow, C., and Levine, R. L. (2004) *Free. Radic. Biol. Med.* **36,** 938–942
12. Gueven, N., Luff, J., Peng, C., Hosokawa, K., Bottle, S. E., and Lavin, M. F. (2006) *Free Radic. Biol. Med.* **41,** 992–1000
13. Rotman, G., and Shiloh, Y. (1997) *Cancer Surv.* **29,** 285–304
14. Reichenbach, J., Schubert, R., Schindler, D., Muller, K., Bohles, H., and Zielen, S. (2002) *Antioxid. Redox Signal.* **4,** 465–469
15. Watters, D. J. (2003) *Redox Rep.* **8,** 23–29
16. Barzilai, A., and Yamamoto, K. (2004) *DNA Repair* **3,** 1109–1115
17. Wong, P. K. Y., and Lynn, W. S. (1997) *J. Immunol. Immunopharmacol.* **17,** 30–35
18. Wang, X. F., and Cynader, M. S. (2000) *J. Neurochem.* **74,** 1434–1442
19. Takuma, K., Baba, A., and Matsuda, T. (2004) *Prog. Neurobiol.* **72,** 111–127
20. Liu, N., Stoica, G., Yan, M., Scofield, V. L., Qiang, W., Lynn, W. S., and Wong, P. K. Y. (2005) *Lab. Investig.* **85,** 1471–1480
21. Gosink, E. C., Chong, M. J., and McKinnon, P. J. (1999) *Cancer Res.* **59,** 5294–5298
22. Molofsky, A. V., He, S., Bydon, M., Morrison, S. J., and Pardal, R. (2005) *Genes Dev.* **19,** 1432–1437
23. Pardal, R., Molofsky, A. V., He, S., and Morrison, S. J. (2005) *Cold Spring Harbor Symp. Quant. Biol.* **70,** 177–185
24. Barlow, C., Hirotsune, S., Paylor, R., Liyanage, M., Eckhaus, M., Collins, F., Shiloh, Y., Crawley, J. N., Ried, T., Tagle, D., and Wynshaw-Boris, A. (1996) *Cell* **86,** 159–171
25. Lin, Y. C., Chow, C. W., Yuen, P. H., and Wong, P. K. Y. (1997) *J. Neurovirol.* **3,** 28–37
26. Lee, Y., Chong, M. J., and McKinnon, P. J. (2001) *J. Neurosci.* **21,** 6687–6693
27. Shikova, E., Lin, Y. C., Saha, K., Brooks, B. R., and Wong, P. K. Y. (1993) *J. Virol.* **67,** 1137–1147
28. Yan, M., Zhu, C., Liu, N., Jiang, Y., Scofield, V. L., Riggs, P. K. Y., Qiang, W., Lynn, W. S., and Wong, P. K. Y. (2006) *Free. Radic. Biol. Med.* **41,** 640–648
29. Lloyd, A. C. (2006) *J. Biol.* (*Bronx N. Y.*) **5,** 13
30. Collado, M., Blasco, M. A., and Serrano, M. (2007) *Cell* **130,** 223–233
31. Wen-Sheng, W. (2003) *Oncogene* **22,** 955–963
32. Bartov, O., Sultana, R., Butterfield, D. A., and Atlas, D. (2006) *Brain Res.* **1069,** 198–206
33. Moors, M., Cline, J. E., Abel, J., and Fritsche, E. (2007) *Toxicol. Appl. Pharmacol.* **221,** 57–67
34. Vonlanthen, S., Heighway, J., Altermatt, H. J., Gugger, M., Kappeler, A., Borner, M. M., van Lohuizen, M., and Betticher, D. C. (2001) *Br. J. Cancer* **84,** 1372–1376
35. Voncken, J. W., Schweizer, D., Agaard, L., Sattler, L., Jantsch, M. F., and von Lohuizen, M. (1999) *J. Cell Sci.* **112,** 4627–4639
36. Min, J., Zhang, Y., and Xu, R. M. (2003) *Genes Dev.* **17,** 1823–1828
37. Yang, Y., and Herrup, K. (2005) *J. Neurosci.* **25,** 2522–2529
38. Maragakis, N. J., and Rothstein, J. D. (2006) *Nat. Clin. Pract. Neurol.* **2,** 679–689
39. Vargas, M. R., Johnson, D. A., Sirkis, D. W., Messing, A., and Johnson, J. A. (2008) *J. Neurosci.* **28,** 13574–13581
40. Nagai, M., Re, D. B., Nagata, T., Chalazonitis, A., Jessell, T. M., Wichterle, H., and Przedborski, S. (2007) *Nat. Neurosci.* **10,** 615–622
41. Otani, N., Nawashiro, H., Fukui, S., Oigawa, H., Ohsumi, A., Toyooka, T., Shima, K., Gomi, H., and Brenner, M. (2006) *J. Clin. Neurosci.* **13,** 934–938
42. Pardo, A. C., Wong, V., Benson, L. M., Dykes, M., Tanaka, K., Rothstein, J. D., and Maragakis, N. J. (2006) *Exp. Neurol.* **201,** 120–130
43. Gamaley, I. A., and Klyubin, I. V. (1999) *Int. Rev. Cytol.* **188,** 203–255
44. Kamsler, A., Daily, D., Hochman, A., Stern, N., Shiloh, Y., Rotman, G., and Barzilai, A. (2001) *Cancer Res.* **61,** 1849–1854
45. Rhee, S. G. (2006) *Science* **312,** 1882–1883
46. Yu, B. P. (1994) *Physiol. Rev.* **74,** 139–162
47. Biswas, S., Chida, A. S., and Rahman, I. (2006) *Biochem. Pharmacol.* **71,** 551–564
48. Benhar, M., Engelberg, D., and Levitzki, A. (2002) *EMBO Rep.* **3,** 420–425
49. Hyslop, P. A., Zhang, Z., Pearson, D. V., and Phebus, L. A. (1995) *Brain Res.* **671,** 181–186
50. Gottfried, C., Tramontina, F., Goncalves, D., Gonçalves, C. A., Moriguchi, E., Dias, R. D., Wofchuk, S. T., and Souza, D. O. (2002) *Mech. Ageing Dev.* **123,** 1333–1340
51. Serrano, M., Lee, H., Chin, L., Cordon-Cardo, C., Beach, D., and DePinho, R. A. (1996) *Cell* **85,** 27–37
52. Quelle, D. E., Cheng, M., Ashmun, R. A., and Sherr, C. J. (1997) *Proc. Natl. Acad. Sci. U. S. A.* **94,** 669–673
53. Ivanchuk, S. M., Mondal, S., Dirks, P. B., and Rutka, J. T. (2001) *J. Neurooncol.* **51,** 219–229
54. Bruggeman, S. W., Valk-Linbeek, M. E., van der Stoop, P. P., Jacobs, J. J., Kieboom, K., Tanger, E., Hulsman, D., Leung, C., Arsenijevic, Y., Marino, S., and van Lohuizen, M. (2005) *Genes Dev.* **19,** 1438–1443
55. Burgoyne, J. R., Madhani, M., Cuello, F., Charles, R. L., Brennan, J. P., Schröder, E., Browning, D. D., and Eaton, P. (2007) *Science* **317,** 1393–1397